VISIBLE RANGE POLARIZED IMAGING FOR HIGH RESOLUTION TRANSVERSE BEAM SIZE MEASUREMENT AT SOLEIL

M. Labat*, A. Bence, A. Berlioux, B. Capitanio, G. Cauchon,
J. Da Silva, N. Hubert, D. Pédeau, M. Thomasset
Synchrotron SOLEIL, Gif-sur-Yvette, France

Abstract

SOLEIL storage ring is presently equipped with three diagnostics beamlines: two in the X-ray range (pinhole cameras) and one in the visible range. The visible range beamline relies on a slotted copper mirror extracting the synchrotron radiation from one of the ring dipoles. The extracted radiation is then transported down to a dedicated hutch in the experimental hall. Up to now, this radiation was split into three branches for rough monitoring of the beam transverse stability, bunch length measurements and filling pattern measurements. In the framework of SOLEIL's upgrade, we now aim at developing a new branch for high resolution beam size measurement using polarized imaging. This work presents the various modifications recently achieved on the beamline to reach this target, including a replacement of the extraction mirror, and preliminary results towards transverse beam size measurement.

INTRODUCTION

SOLEIL storage ring presently delivers synchrotron radiation to 29 beamlines. The stability of the delivered photon beams, a main figure of merit for users, relies on an accurate monitoring of the electron beam orbit and electron beam size / emittance at users source points. Presently, two beamlines in the X–ray range are dedicated to beam transverse size diagnostics, relying on pinhole camera systems. The high-resolution pinhole cameras' measurements are used in a feedback loop to maintain the vertical emittance within $\pm 5\%$. Despite the high reliability of those pinhole cameras, it would be reassuring to have an additional beam size measurement based on a different technique for redundancy and further verification of the absolute emittance value. This is the main reason why, for three years, we have been working on the upgrade of our third diagnostics beamline, the MRSV beamline (Visible Synchrotron Radiation Monitor) in the visible range, to implement an additional high–resolution beam size measurement based on π polarized imaging [2]. This development also turns to be of high interest in the perspective of SOLEIL–II: it might be indeed the only way to obtain, together with a pinhole camera, two beam size measurements with two different dispersion functions for energy spread retrieval. It is finally worth mentioning that, thanks to the high available photon flux on the MRSV beamline, beam size measurements should be achievable down to very low, ≈ 1 mA, currents (whereas pinhole cameras can't be operated below 10 mA) and could be run above the kHz

range at 500 mA (whereas pinhole cameras are limited to the 10 Hz range). This work presents the main steps of the upgrade of the MRSV beamline together with preliminary results.

GENERAL LAYOUT

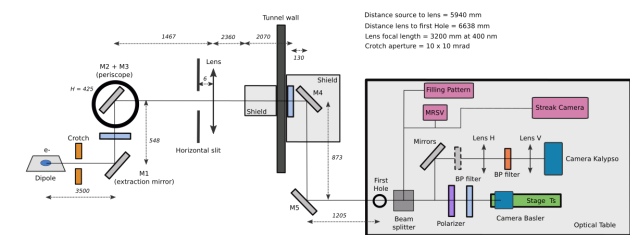The experimental layout of the MRSV beamline is presented in Fig. 1.

Figure 1: Layout of the MRSV beamline.

The Synchrotron Radiation (SR) of one of the ring dipoles (ANS-C01) is extracted using a slotted mirror, the slot being centered on the beam axis to let SR X–rays go through. The collected photons have a wavelength λ spanning from ≈ 190 to nearly 900 nm. The SR is then transported via a set of mirrors, including a periscope, down to a hutch in the experimental hall. On the beam path inside the tunnel are successively placed a slit and a lens. At the arrival on the optical bench in the hutch, the SR is split into several branches.

Initially, three branches were implemented (see pink boxes in Fig. 1): one with a fast diode for filling pattern measurement, one with a Streak Camera for bunch length measurement and one with a standard Ethernet camera for a coarse imaging of the beam at the source point. We added two new branches to test higher resolution / higher speed imaging systems for beam size retrieval at the source point of the MRSV beamline. We will focus in the following on the high resolution branch (see bottom branch in Fig. 1).

NEW EXTRACTION MIRROR

The initial extraction mirror was already a slotted mirror but without optimized cooling system. In standard operation at 500 mA, when the mirror was inserted in the *slot–insertion* mode, i.e. with its slot centered vertically on the SR fan, its temperature was continuously raising without reaching an equilibrium, preventing its safe use. A new design was therefore optimized in–house in order to guarantee a fast thermal equilibrium of the mirror at 500 mA and to ensure a surface

_____

* marie.labat@synchrotron-soleil.fr

distortion at this equilibrium below $\lambda/2$ with $\lambda=400$ nm. The final system is shown in Fig. 2. The mirror was manufactured by Kircheim Optics company. It is a 15 mm thick bulk of Copper (CuC_2) drilled by a 5.6 mm height slot. Its incident surface is coated with an enhanced Aluminium deposit allowing high reflectivity down to 200 nm. The mirror was characterized by the Optics Group of SOLEIL upon its receipt. The measurements revealed that the flatness was below 200 nm peak–to–valley, the rugosity less than 3 nm even nearby the slot edges and the overall radius of curvature above 15 km, i.e. fully beyond the initial specifications. At the rear of the mirror, a Macor ceramic plate enables to hold a set of height thermocouples of K type. Six of them are placed all around the slot and aligned in order to go slightly beyond the mirror shadow (by 0.3 mm) and intercept the SR fan. They enable the accurate vertical centering of the mirror on the SR fan. The other two thermocouples are placed at the bottom of the ceramic plate and aligned to go slightly beyond the mirror bottom shadow. Those are used for a *surf–insertion* of the mirror (the mirror is *surfing* on the top–half of the SR fan to allow larger orbit deviations during machine studies). Two additional thermocouples are forced into the edge faces of the mirror in order to probe the mirror body temperature.
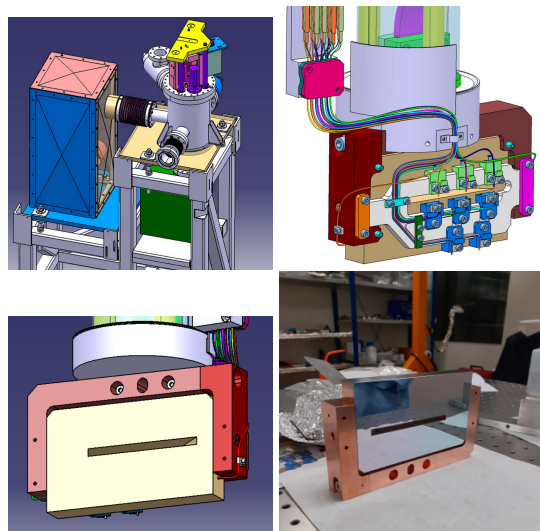

Figure 2: 3D views of the new extraction mirror and picture of the mirror before its installation.

The mirror is then gripped in a copper fork in order to minimize possible stress distortions. Thin (30 μm) Indium foils were inserted in between the mirror edge faces and the fork to optimize the heat transfer from the mirror to the fork. The fork is itself screwed on the bottom tap of an inverted bellow (air inside, vacuum outside). Inside this bellow, a rod enables to insert/extract the mirror while a large copper braid finalizes the heat transfer from the fork to the outside of the vacuum chamber housing the mirror, i.e. to the tunnel ambient air. The mirror is therefore simply but efficiently air–cooled. In standard operation, the total incident power on the mirror is expected to be 3.5 W (possibly 4.5 W at maximum

orbit deviation). According to thermal simulations, in these conditions, the mirror is expected to reach an equilibrium temperature of 34°C and to suffer a maximum distortion of 300 nm peak-to-valley nearby the slot.

The mirror was installed in January 2022. After few hours of conditioning, it was inserted in the *slot–insertion* mode at 500 mA: the measured equilibrium temperature, reached within few tens of minutes, was 33°C, in excellent agreement with calculations, while no significant distortion of the radiation wavefront could be observed downstream while increasing the current, indicating negligible distortion of the mirror surface. Thanks to this main upgrade, it is now possible to operate the MRSV beamline with the extraction mirror in *slot–insertion* mode in standard operation at 500 mA.

NEW BEAMLINE COMPONENTS

Unfortunately, the upgrade of the extraction mirror was insufficient to achieve high resolution beam size measurements. Other beamline components too needed a refurbish/upgrade.

Figure 3: Pictures of the UHV Fused Silica window. Left: after 10 years of operation. Right: after 2 years of operation.

UHV Viewport

The first optical component downstream of the extraction mirror is a viewport ensuring the transition between the Ultra–High–Vacuum (UHV) of the chamber housing the extraction mirror and the ambient air of the tunnel housing the downstream components of the beamline. Since the first hours of the MRSV beamline, the viewports successively installed are made of standard Fused Silica. Recently, we realized that a couple of years of operation were enough to seriously damage the viewport as shown in Fig. 3: a white *snow* is deposited on the air–side of the viewport, nearby the mirror slot edges projection, and a whitening of the viewport is observed all over the surface where the collected SR is transmitted. Such damage is bearable during several years for one using the photon flux, but becomes unbearable within less than one year to exploit the SR wavefront. The Optics Group of SOLEIL investigated the origin of this fast damage and recently reached conclusions of high interest. The damage seems to come from two processes. (1) Inside the viewport, water molecules can get trapped during the annealing process of the Fused Silica. The SR UV photons would then dissociate those molecules and create trapped Hydrogen molecules responsible for the whitening of the viewport. (2) On the outer/air side of the viewport, the exiting SR UV photons (at $\lambda <240$ nm, probably more specifically at $\lambda=185$ nm) convert the oxygen in the air into atomic oxygen through photolysis, leading to the production of ozone. The

ozone would then itself be transformed through photolysis by the SR UV photons at $\lambda < 350$ nm. The products of all those reactions are extremely oxidizing, especially for metals, and cause a localized de–polishing of the window surface in addition to a white deposit. This viewport degradation is of great harm for a high–resolution beam size measurement, creating a diffraction pattern in the image plane. Our observations showed that our damaged window was transmitting indeed as if there was a 1 mm thick line obstacle on the beam path (at the lens location). Building on those results, two actions are under way: the purchase of new type of windows to reduce the in–bulk effect and a main beamline update to enclose the light path under primary vacuum down to the image plane to reduce the exit surface (*snow*) effect. Regarding new windows, we systematically compared all available options from manufacturers. It came out that three types of alternative substrates could be more transmissive in the 180–250 nm range: CaF_2, MgF_2 and EUV Grade Fused Silica. CaF_2, MgF_2 windows are crystalline glass, i.e. potentially more pure (without trapped water molecules), and can transmit up to $\lambda = 1000$ nm. But they are significantly more expensive than EUV Grade Fused Silica and slightly less transmissive in the 180–200 range. EUV Excimer Grade Fused Silica windows, initially optimized for excimer laser users, are now available with homogeneity grade A and inclusion class 0 with excellent surface quality. Two items were already ordered and should be installed before the end of the year.

Periscope Mirrors

A few centimeters downstream of the viewport, a periscope lowers the SR beam out of the electron beam orbit plane. The two mirrors mounted on the periscope are made of a Zerodur substrate coated with Silver. But those mirrors are also suffering a fast damaging as shown in Fig. 4. There is no *snow* deposited since the shortest wavelengths do not get through more than a few centimeters of air, but the mirrors are depolished all over the SR incident surface. This depolishing starts affecting the SR wavefront wihtin a year of operation. To try increasing the lifetime of those mirrors, we decided to test a new coating. A new pair of enhanced UV Aluminium coated mirrors was installed during summer shutdown. Even if this coating is confirmed to be more resistant to UV radiation, the enclosing of the periscope under vacuum might remain mandatory.
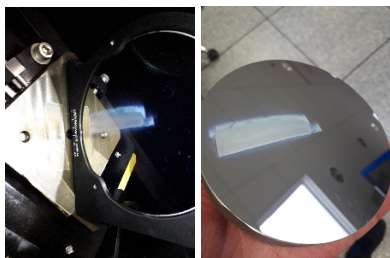

Figure 4: Pictures of the Silver coated periscope mirrors after several years of operation.

Other Optical Components

Still inside the tunnel, a motorized slit enables to control the horizontal collection angle θ_x from 0 up to 10 mrad. Immediately following this slit, a $f=3200$ mm cylindrical lens refocusses the SR with non–negligible chromatic effects. This lens is indeed 7 mm thick on–axis and made of Fused Silica. Up to now, no degradation of the lens could be observed. After passing through a thick shielding via a 45° incidence mirror, the SR reaches the optical table of the diagnostics hutch. Using a few beamsplitters as shown in Fig. 1, the SR is dispatched towards five branches. The last bottom branch is the one dedicated to attempt high resolution beam size measurements. According to preliminary simulations, the highest resolutions are expected to be reached using π polarized SR. A transmission type linear polarizer can therefore be mounted on a rotation stage. The SR is also monochromatized with a bandpass filter of 5 nm–fwhm centered at $\lambda = 405$ nm. The SR transverse distribution in the image plane is finally recorded with a CMOS camera (acA1920-50 gm from Basler) which pixel pitch is 5.86 µm.

BEAMLINE MODELLING

To achieve a high resolution beam size retrieval from π polarized imaging, an accurate modelling of the beamline is mandatory. We used for that the SRW (*Synchrotron Radiation Workshop*) code [1]. The beamline is modelled taking into account the crotch absorber aperture, the extraction mirror slit, the aperture of the horizontal slit, the focussing of the lens and the polarizer transmission. The 2D SR wavefront (in x and y the transverse coordinates) is computed in multi–electron mode –to take into account the finite electron beam emittance at source point– for a single photon wavelength $\lambda = 405$ nm (we checked that the 5 nm–fwhm bandpass filter allowed to work in this monochromatic approximation).

PRELIMINARY IMAGING RESULTS

Before addressing beam size measurements strictly speaking, major efforts were made to obtain an excellent agreement between simulated and measured transverse distributions both over a large field of view and as a function of many parameters (polarizer angle, distance to image plane, horizontal collection angle, vertical position of the extraction mirror, etc..). Those long term efforts revealed to be extremely helpful to identify the faulty components of the beamline (as mentioned above). For the sake of simplicity, only two scans are presented here, scans that we however believe to be the most illustrative of the quality of our new extraction mirror and of the consequent level of agreement we could reach up to now. The first scan, presented in Fig. 5, is versus D the distance from the lens to the camera. The second scan, presented in Fig. 6, is versus θ_x the horizontal collection angle. In both scans, measurements (bottom line) are compared to simulations (upper line) using the extraction mirror in (a) *full–insertion* and (b) *slot–insertion* mode, without polarizer, and for a collection angle $\theta_x = 0.5$ mrad

11th Int. Beam Instrum. Conf.   IBIC2022, Kraków, Poland   JACoW Publishing

ISBN: 978-3-95450-241-7   ISSN: 2673-5350   doi:10.18429/JACoW-IBIC2022-TUP19

allowing to observe the diffraction pattern from the horizontal slit. For mirror safety reasons, experimental data were recorded at I=1.7 mA to avoid any mirror damage / distortion. The agreement between measurements and simulations is excellent, mainly resulting from the high quality of the optics.
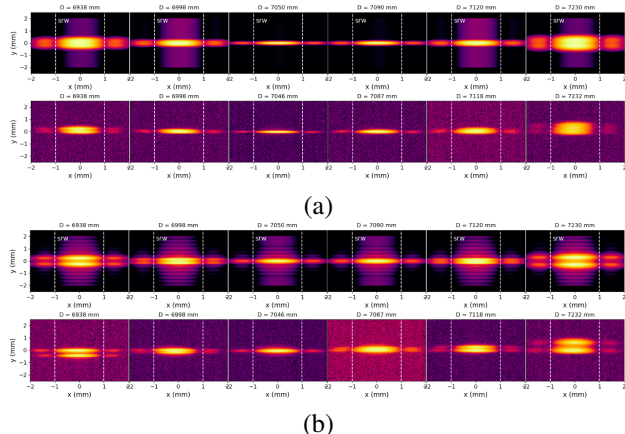

(a)

(b)

Figure 5: Intensity distributions versus D using the extraction mirror in (a) *full–insertion* mode and (b) *slot–insertion* mode. In (a) and (b): (upper line) simulations, (bottom line) measurements. Main conditions: θ_x=0.5 mrad, θ_y=10 mrad, no polarizer, λ=405 nm. Experimental parameters: I=1.7 mA. Simulation parameters: f_x=3194 mm, f_y=3227 mm.
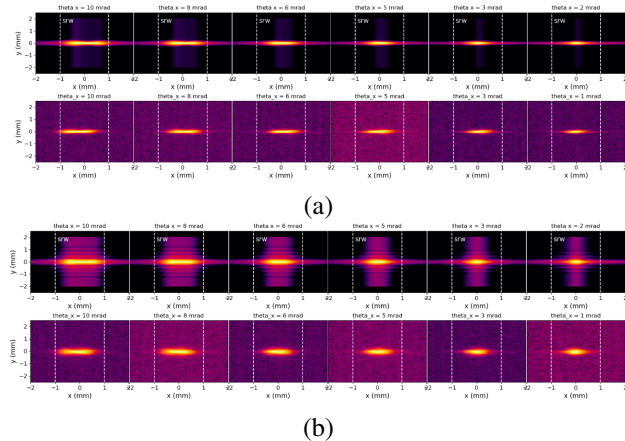

(a)

(b)

Figure 6: Intensity distributions versus θ_x using the extraction mirror in (a) *full–insertion* mode and (b) *slot–insertion* mode. In (a) and (b): (upper line) simulations, (bottom line) measurements. Main conditions: D=7.06 m, θ_y=10 mrad, no polarizer, λ=405 nm. Experimental parameters: I=1.7 mA. Simulation parameters: f_x=3194 mm, f_y=3227 mm.

TOWARDS BEAM SIZE MEASUREMENTS

Heartened by the good agreement between measurements and simulations, we are now about to move on to strictly speaking beam size measurements. According to SRW, the highest resolution in terms of vertical beam size measurements should be reached using a vertical (π) polarization. A preliminary scan versus D in π polarization and using the mirror in *slot–insertion* mode is shown in Fig. 7. The once more excellent agreement between simulations and measurements allow us to be confident for close future absolute and high–resolution beam size measurements.
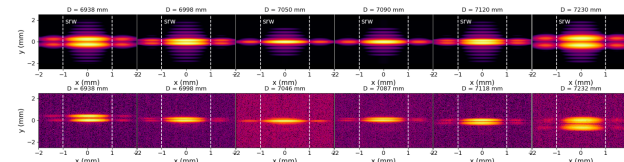

Figure 7: Intensity distributions versus D using the extraction mirror in *slot–insertion* mode. (Upper line) simulations, (bottom line) measurements. Main conditions: θ_x=0.5 mrad, θ_y=10 mrad, vertical polarizing, λ=405 nm. Experimental parameters: I=1.7 mA. Simulation parameters: f_x=3194 mm, f_y=3227 mm.

CONCLUSION

We presented here the recent developments performed on our visible range diagnostics beamline.

We recently realized how fast our optics were being damaged and we reported here the fundamental mechanisms that we believe to be leading to this fast damaging. Relying on this new knowledge, and strongly encouraged by the perspective of SOLEIL upgrade, we are now working on the improvement of our optics lifetime.

We also reported on systematic comparisons between measured and simulated radiation distribution in the beamline image plane. The excellent agreement recently reached appears very reassuring for a moving on towards absolute beam size retrieval.

We could also recently confirm that, thanks to the high SR photon flux, π polarized imaging based beam size measurements are feasible down to $\approx$ 1.7 mA, i.e. in a low current range where pinhole cameras are inoperable from lack of signal. This also means that at 500 mA, π polarized imaging can be run at a much higher repetition rate than pinhole cameras. The door seems opened for high–resolution and high repetition rate ($>$ 1 kHz) beam size measurements in the visible range.

REFERENCES

[1] O. Chubar and P. Elleaume, "Accurate and Efficient Computation of Synchrotron Radiation in the Near Field Region", in *Proc. EPAC'98*, Stockholm, Sweden, Jun. 1998, paper THP01G, pp. 1177–1179.

[2] A. Andersson *et al.*, "Determination of a small vertical electron beam profile and emittance at the Swiss Light Source", *Nucl. Instrum. Methods Phys. Res., Sect. A*, vol. 591, pp. 437–446, 2008. doi:10.1016/j.nima.2008.02.095